Bulletin of the Seismological Society of America, Vol. 95, No. 3, pp. 818–832, June 2005, doi: 10.1785/0120040019

Mount Hood Earthquake Activity: Volcanic or Tectonic Origins?

by J. Jones and S. D. Malone

Abstract On 29 June 2002, a M_D 4.5 earthquake occurred 4.6 km south of Mount Hood, Oregon. More than 200 small aftershocks ($M_D \leq 3.8$) occurred between 29 June and 15 August 2002, by which time seismicity returned to background levels. We analyze well-constrained earthquakes from the summer 2002 sequence near Mount Hood, recorded by the Pacific Northwest Seismic Network (PNSN), and well-constrained, small earthquakes ($M_D \leq 3.5$) recorded by the PNSN between 1986 and 2002. We apply waveform cross-correlation to selected events, establish a one-dimensional *P*-wave velocity model, and relocate the entire catalog by using the double-difference algorithm of Waldhauser and Ellsworth (2000). We find that earthquakes before 2002 occur in four distinct clusters: (A) a well-defined linear feature, striking N15E, about 5 km south of the summit, (B) a linear feature, trending northwest–southeast a few kilometers south of group A, (C) a few tight clusters located about 9 km south-southwest of the summit, and (D) a small cluster beneath the summit. Earthquakes in group D do not appear to lie on a fault and may relate to volcanic activity. However, almost all earthquakes in the 2002 swarm occur in group A, south of the summit, at depths similar to earthquakes from previous swarms. First-motion fault-plane solutions from the mainshock and largest aftershocks have normal mechanisms, and solutions from well-constrained aftershocks have normal to oblique normal mechanisms. This is consistent with the apparent strike of the feature south of Mount Hood's summit and is similar to focal mechanisms of older earthquakes in group A. *b*- and *p*-values for the summer 2002 earthquakes resemble a tectonic mainshock-aftershock sequence. We interpret these earthquakes as the northernmost example of Basin-and-Range seismicity yet recorded and conclude that the Mount Hood earthquakes do not yet suggest potential for volcanic unrest.

Introduction

Mount Hood, a late Pleistocene to Holocene stratovolcano in north-central Oregon, is one of fifteen major composite stratovolcanoes in the Cascade Range. It is the only Oregon volcano with historic eruptive activity: Its last significant eruption ended around 1800 and produced such prominent geographic features as the Crater Rock dacite plug dome, the Old Maid Flat mud flow, and debris fans that cover the mountain's south flank (Wise, 1969; Friedman *et al.*, 1982; Williams *et al.*, 1982). Minor summit explosions were reported by settlers from 1856 to 1865, often accompanied by reports of a visible glow around the summit area (Folsom, 1970). No eruptive activity has been reported since that time.

Several pieces of evidence suggest that, though currently quiescent, Mount Hood is not extinct. Williams *et al.* (1982) report a 200-m-thick deposit of near-vent andesite at a drill hole adjacent to Mount Hood's lower west flank and suggest that its volcanic system is in the early stages of development. Friedman *et al.* (1982) found that heat loss due to cooling of the dacite dome was insufficient to explain the heat flux of Mount Hood's fumaroles, and suggest a deep-seated heat source. Williams *et al.* (1982) report observing a thermal gradient of 60°C/km, implying that partial melt must occur no deeper than 15 km. These pieces of evidence all point toward a magma system under Mount Hood.

At the same time, however, none of the previous seismic studies at Mount Hood. (Weaver *et al.*, 1982; Leaver, 1984) detected a low-velocity zone consistent with the existence of a shallow magma chamber. Similarly, gravity analyses of the Mount Hood region (Couch and Gemperle, 1979) failed to detect a significant gravity anomaly, such as that which a large magma chamber would produce.

To place constraints on the origins of a recent earthquake sequence and relate it to earlier swarms, we analyze the spatial distribution, relative locations, and focal mechanisms of Mount Hood microearthquakes, using cross-correlation and double-difference earthquake location, then examine the Mount Hood catalog more closely using statistical analysis.

Seismic Monitoring and Historic Seismicity

A review of historic seismicity for the Oregon cascades, through 1958, is given in Berg and Baker (1963). Although locations for most of these earthquakes are questionable, none of these historic earthquakes were located near Mount Hood. Before 2002, the largest earthquake recorded near Mount Hood was a M_D 4.0 earthquake on 13 December 1974 located 14 km south-southeast of the Mount Hood summit (Rite and Iyer, 1981). However, because the Pacific Northwest was not well instrumented at the time, the location error is quite large, and the earthquake may have occurred much closer to the volcano.

The first detailed study of Mount Hood was a short-term experiment using a temporary array of high-frequency ($f_0 =$ 25 Hz) seismometers deployed about 7.5 km to the north of Mount Hood summit (Westhusig, 1973). This survey recorded 53 local events, with magnitudes between -1.7 and $+1.8$. About 80% of these were located south of the array and had depths between 5 and 10 km, which are consistent with catalog depths for more recent Mount Hood earthquakes. Most of these events were located beneath the summit of Mount Hood.

In 1977, a multidisciplinary study was conducted at Mount Hood to evaluate the geothermal potential of a typical Cascade volcano (Williams *et al.*, 1982). As part of this study, a temporary, 16-station network of short-period seismometers was deployed in the Mount Hood region, from November 1977 to December 1978 (Green *et al.*, 1979; Weaver *et al.*, 1982). This network recorded only 10 locatable, local events. Most occurred roughly beneath the summit, at shallow depths, with magnitudes $M_D < 2.0$. One larger event occurred, with an estimated magnitude M_D 3.4. First-motion focal mechanisms were computed for five of these events. Four showed strike-slip first motions, whereas one was oblique normal.

The Pacific Northwest Seismic Network (PNSN) has monitored seismicity in the Mount Hood area since the summer of 1980. Since 1982, Mount Hood has been monitored by a network of five telemetered, short-period, vertical seismograph stations, all within 30 km of the summit (Fig. 1) with several additional, more distant stations contributing data for larger events.

Since 1980, the PNSN has recorded more than 900 microearthquakes ($M_D \leq 3.0$) near Mount Hood (Fig. 2). Detection capabilities have remained roughly constant for Mount Hood earthquakes since 1986, but 76% of the earthquakes recorded near Mount Hood have occurred since 1997 (Fig. 3). This clearly shows that the rate of seismicity is increasing. Earthquakes occur in two diffuse clouds, whose relation to volcanic processes and/or tectonic features has been difficult to determine. One of these, a cloud trending southeast from beneath the summit, apparently includes some earthquakes underneath the summit itself and contains the vast majority of Mount Hood earthquakes. The other, a feature to the southwest, also trends generally northwest–southeast, but is far less seismically active. Catalog depths for events show no obvious patterns that could relate them to volcanic activity.

Three temporary deployments have occurred at Mount Hood since 1980 including a short-period seismic station in July 1980, three short-period stations in early January 1999, and a temporary CMG-40T broadband station (HDM; Fig. 1) in July 2002. Each of these deployments was in response to increased seismicity beneath the volcano. The temporary broadband station of July 2002 was replaced with a telemetered broadband station in November 2002 and is now a permanent part of the PNSN (Fig. 1).

History of Mount Hood Earthquake Swarms

Small swarms, ranging from a few earthquakes to several tens of earthquakes, have been detected at Mount Hood since permanent seismic monitoring began. Most Mount Hood events occur during these swarms, which last from one to several days and are followed by periods of quiescence, ranging from several weeks to tens of months (Fig. 4). Swarms exhibit many features of volcanotectonic (VT) earthquakes (Lahr *et al.*, 1994). For example, all Mount Hood microearthquakes exhibit spectral characteristics and phases typical of tectonic earthquakes. They exhibit clear *P* and *S* phases, and frequency content up to 15 Hz at local distances. No low-frequency earthquakes or episodes of volcanic tremor have ever been recorded near Mount Hood. In addition, the temporal evolution of Mount Hood earthquake sequences is typical of VT earthquake swarms: the largest earthquake in a sequence usually does not occur at the beginning of the swarm, in contrast to typical mainshock-aftershock sequences (Fig. 5). Additionally, first-motion focal mechanisms typically show normal faulting, in contrast to thrust-faulting mechanisms seen elsewhere in northern Oregon (Thomas *et al.*, 1996). Thus, a different stress regime must be responsible for Mount Hood earthquakes than for other nearby crustal events. Therefore, although individual earthquakes have characteristics that are similar to tectonic earthquakes, their temporal evolution and focal mechanisms suggest that they might be related to volcanic processes rather than regional tectonic stress.

The Summer 2002 Earthquake Sequence

On 29 June 2002 (UTC) a M_D 4.5 earthquake occurred 4.6 km south of Mount Hood. One small (M_D 1.1) foreshock was detected approximately 2 min before the main event. More than 200 small aftershocks ($M_D \leq 3.8$) occurred between 29 June and 18 August, after which seismicity returned to background levels. PNSN catalog locations placed most aftershocks in a diffuse cloud 4–7 km south of the Mount Hood summit, near most of the catalog earthquake locations. For convenience, we refer to this sequence hereafter as the "summer 2002 earthquake swarm." Unlike previous earthquake swarms, the temporal evolution of these

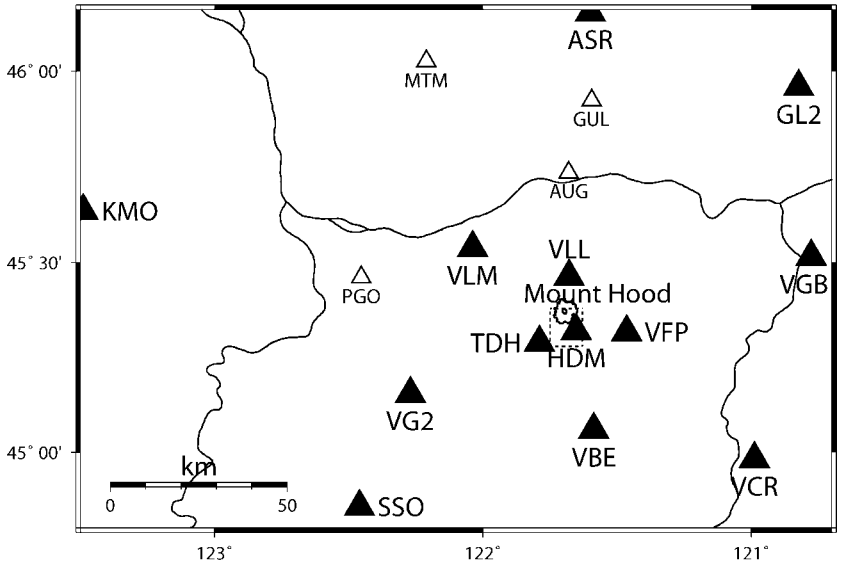

Figure 1. Map showing station names and PNSN network geometry. All stations use permanent short-period vertical component sensors, except the temporary station HDM. Position of Mount Hood is indicated by text and 1000-m contour lines. Solid black triangles indicate stations used in this study. Open triangles represent unused stations. Dashed lines indicate region of detailed epicenter maps.

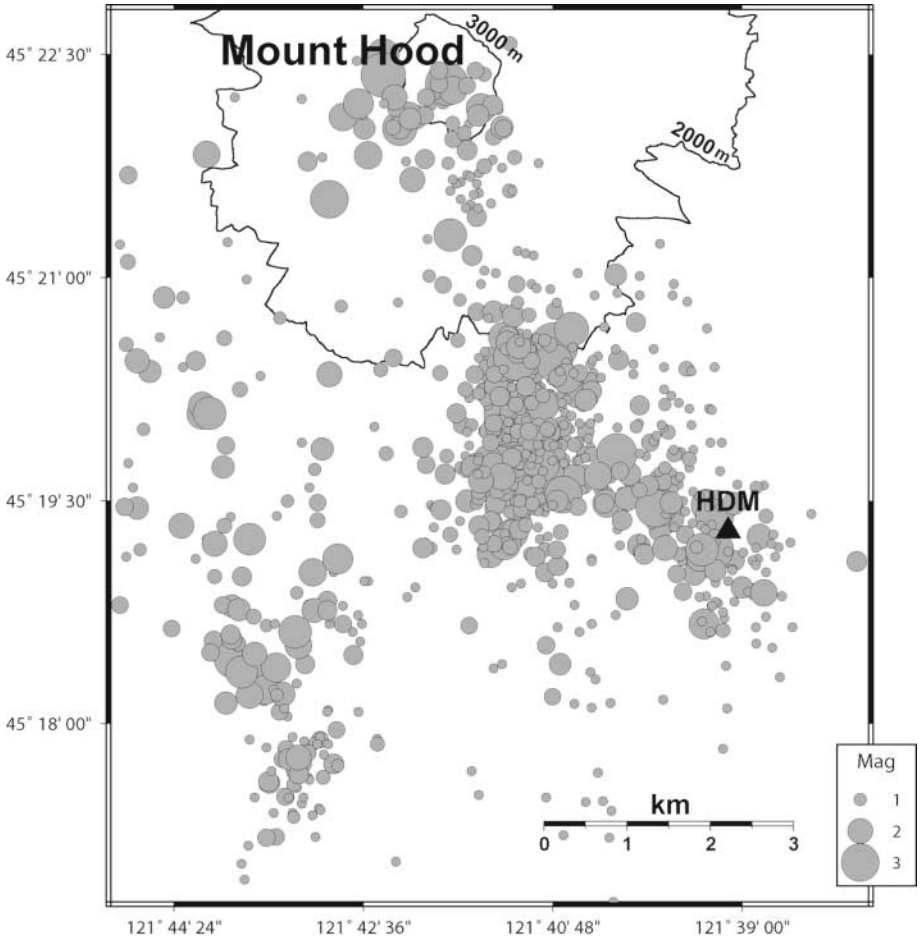

Figure 2. PNSN catalog epicenters of earthquakes recorded near Mount Hood, January 1980 through August 2002. Earthquakes are represented by gray circles. Epicenter size is scaled according to coda magnitude. Contour lines show 2000-m and 3000-m above sea level, as indicated.

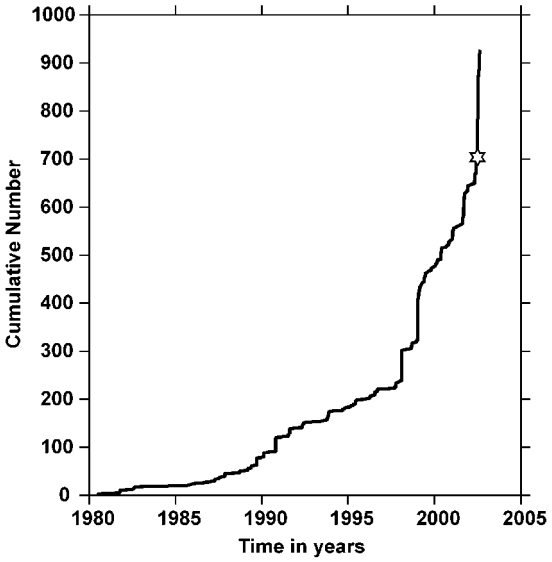

Figure 3. Cumulative number of earthquakes recorded at Mount Hood, as a function of time, January 1980 through August 2002. Star represents the 29 June 2002, M_D 4.5 earthquake.

earthquakes seems more typical of mainshock-aftershock sequences (Fig. 6). However, some ambiguity remains because of the lack of significant historic earthquakes ($M_D > 4.0$), the departure from previous temporal patterns, and the proximity to a historically active volcano.

Data Selection

All stations used in this study sample data at 100 Hz. With the exception of the temporary broadband station HDM, all sensors are Mark products vertical component L-4 seismometers ($f_0 = 1$ Hz). The Mount Hood catalog includes more than 900 earthquakes, of $-0.9 < M_D \leq 4.5$, as of 31 August 2002. More than 200 of these occurred during the summer 2002 earthquake swarm. We selected earthquakes and stations for further analysis based on quality, uniform station coverage, and number of traces.

No event was used unless six or more phases were recorded at five or more of the selected stations. To minimize location errors associated with large azimuthal gaps, events were restricted to those with either two or more catalog *S* arrivals or those with azimuthal gaps of less than 150°. To ensure consistent station coverage, events were restricted to those with trace data at four or more stations within 50 km of Mount Hood, including the temporary station HDM (Fig. 1). Because few PNSN stations were installed near Mount Hood before the early 1980s, and initial station coverage was subject to occasional large recording gaps, this restricts our analysis to events recorded after 1985. However, note that the PNSN recorded only 28 events at Mount Hood between 1980 and the end of 1986 whose catalog locations are mostly in the more populous cloud. Thus, we expect no biased results from restricting our temporal window.

After applying these selection criteria, the number of events available for detailed study was reduced to 415, or about 40% of the Mount Hood catalog. Most of the rejected events were either too small to pick reliable arrival times at five stations or appeared at too few stations because of station outages.

Stations were selected primarily based on available trace data. The six closest stations to Mount Hood were used (Fig. 1), because their signal-to-noise ratios were very high. Stations farther than 50 km were chosen based on the signal-to-noise ratios of Mount Hood earthquakes with $M_D \geq 1.0$. Stations were only selected if trace data were available for 100 or more of these earthquakes; they were further restricted by requiring that trace data have sufficient signal-to-noise ratio to pick arrival times for at least half the available traces. Stations more than 150 km from Mount Hood were not used.

Cross-Correlation and 1D Velocity Inversion

The method of using waveform cross-correlation to group earthquakes based on waveform similarity is not new. It has been used extensively to relocate earthquakes in volcanic regions. Examples include Rowe *et al.* (2002) for Montserrat, West Indies, Rubin *et al.* (1998) for Kilauea, and Musumeci *et al.* (2002) and Fremont and Malone (1987) for Mount St. Helens. The method works because earthquakes with similar locations and source mechanisms produce similar seismograms at a given station. The technique used in our analysis is based on methods introduced by Van Decar and Crosson (1990) and adapted by Deichman and Garcia-Fernandez (1992) and Dodge *et al.* (1995). The method builds groups of similar waveforms at a seismic station by correlating candidate traces against stacks of previously grouped earthquakes. For each group, the method calculates all possible cross-correlations between pairs of traces and uses a weighted least-squares adjustment procedure to solve for a set of arrival-time corrections most consistent with a set of delays. Details of this method are given in Van Decar and Crosson (1990).

We used the Xadjust waveform cross-correlation program of Dodge *et al.* (1995) to determine relative phase-arrival times. Data were typically filtered with a zero-phase four-pole Butterworth filter, with corner frequencies of 2 and 14 Hz before cross-correlation. However, for some stations, corner frequencies were changed because of problems with persistent site noise.

At all stations, traces were grouped using a narrow (0.6–1.5 sec) window of filtered data containing the *P* arrival. Two traces *i* and *j* are considered similar if their mean cross-correlation coefficient, C_{ij}, is at least 0.85. Correlation window length is shortest at stations closest to earthquake epicenters and is increased for stations at greater distances. At stations KMO, VCR, and VLM, and the temporary station

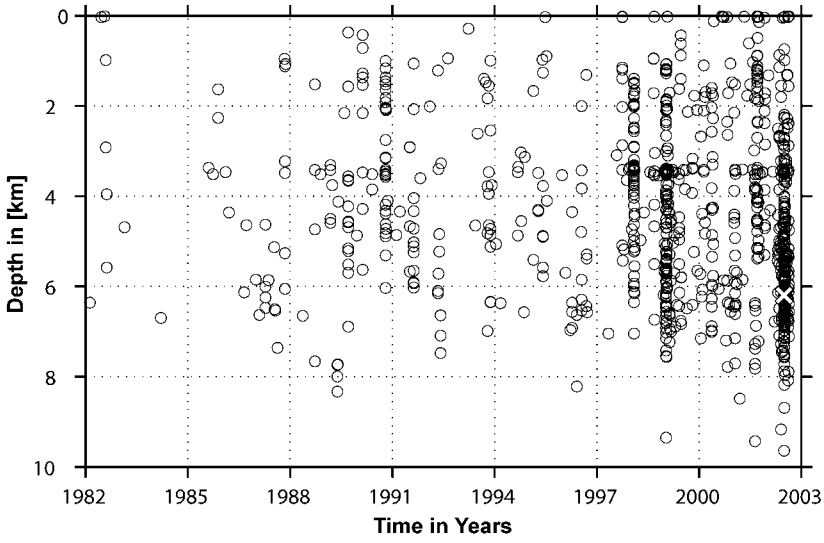

Figure 4. Time-depth plot of earthquakes recorded near Mount Hood. The white "X" designates the 29 June 2002, M_D 4.5 earthquake. Circles represent other events.

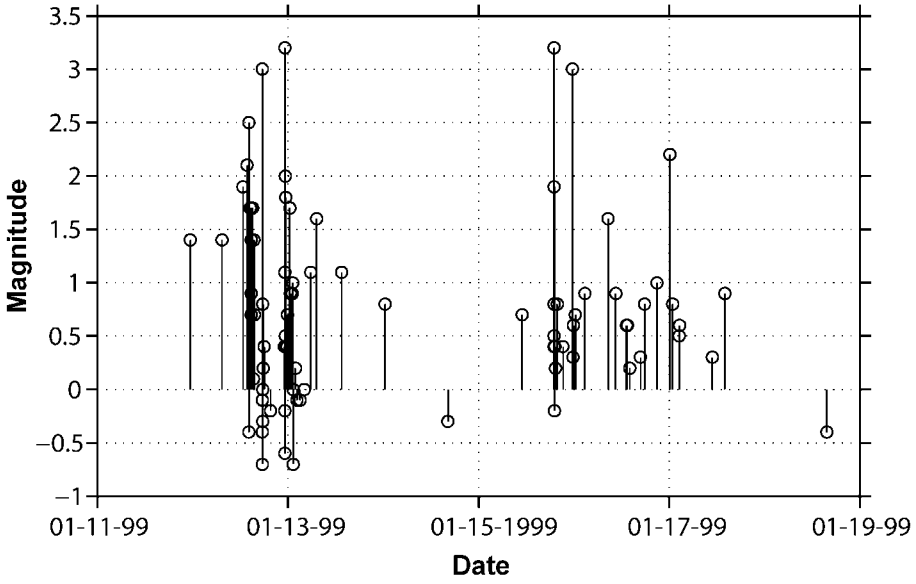

Figure 5. Plot of earthquake magnitudes as a function of time for an earthquake swarm that occurred in early January 1999. The swarm lacks a clear mainshock, and the largest earthquakes do not occur at the beginning of the swarm.

HDM, *S* arrivals were also correlated. Although most analyst picks were relatively consistent at nearby stations, some arrival times at more distant stations shifted by more than 0.1 sec (Fig. 7). At all stations, filtered and raw traces were visually inspected after groups were determined to ensure accuracy. Several traces were removed from the analysis, bringing the number of relocatable events down to 387. A total of 80%–90% of each station's traces were grouped and had picks readjusted, although the number of groups naturally varied from station to station.

Once picks were adjusted, we used *P*-arrival times of all events with trace data at 10 or more selected stations (89 events) to invert for a 1D *P*-wave velocity model and station corrections that minimize rms (Kissling *et al.*, 1994). Because some stations were down for larger events, including the 29 June 2002 mainshock and its largest aftershocks, no earthquake was recorded at all 13 stations, and only a few were recorded at 12. We used the velocity model of Leaver (1984) as an initial starting model, then solved the coupled hypocenter-velocity model problem described by Crosson (1976) using the program Velest of Kissling *et al.* (1994). Figure 8 shows the initial and final velocity models.

Our inverted velocity model differs slightly from that obtained by Leaver (1984). Notably, the minimum 1D model includes a weak low-velocity zone at 4 km depth. A simple jackknife test, wherein one station at a time is removed from the velocity inversion, shows that this layer appears for all stable velocity inversions. We conclude that this low-

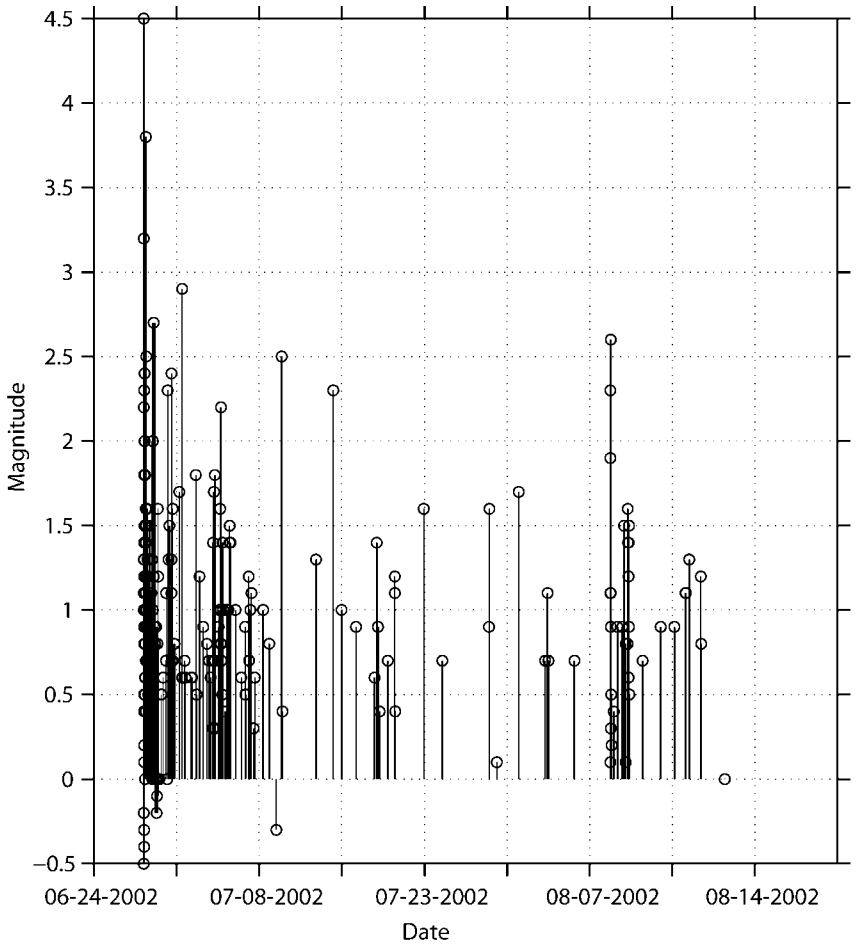

Figure 6. Plot of earthquake magnitudes as a function of time for the earthquakes of June through August 2002, showing the M_D 4.5 main-shock of 29 June.

velocity layer is not an artifact of the stations used. Because the *P*-wave velocity of the lower layer differs from that of the upper layer by $<1\%$, we attach no special significance to this low-velocity zone. However, the presence of any low-velocity zone at a historically active volcano deserves explicit mention.

Earthquake Relocations and Focal Mechanisms

Once a 1D velocity model was established, we obtained double-difference locations for all earthquakes, using the best 1D velocity model to form differential travel-time residuals. We used the hypoDD program of Waldhauser and Ellsworth (2000) to obtain double-difference locations. Both *P*- and *S*-wave arrivals were used, with the assumption $V_s = V_p/1.73$. Because some outliers were included in this analysis, and all Mount Hood events fell within a 100-km^2 area, travel-time pairs were weighted by using residual threshold but not distance. In this way, the relative locations of all events were constrained by all other selected picks. HypoDD successfully relocated 384 events based on cross-correlated picks, as compared with only 360 when run with only catalog picks. Some events were automatically removed by the relocation algorithm once their depths decreased to less than 0 km.

The combination of cross-correlated picks and the best 1D velocity model obtained from Velest leads to considerable refinement of the hypocenters' spatial distribution (Fig. 9). It is clear from Figure 9c that Mount Hood earthquakes occur in four distinct clusters, with only a few outliers: (1) A small cluster of earthquakes occurring beneath the summit, (2) a cluster located about 9 km south-southwest of the summit, along with several multiplets, (3) a linear feature, trending north–south, about 5 km south of the summit, and (4) a well-defined linear "streak" feature, trending northwest–southeast, a few kilometers further south. This clustering is also detected when events are relocated with hypoDD based only on catalog picks (Fig. 9b, d). However, because of difficulties in accurately identifying individual picks, processing catalog picks only forms approximately 60% as many double-difference pairs as for the cross-correlated picks. This means that the relocations obtained from cross-correlation are better constrained than those obtained from catalog picks.

After adjusting the picks, polarities were reassigned by using the adjusted arrival times of traces whose raw data showed an impulsive arrival. We find that re-examining raw data in this way allows for up to 30% more polarity picks at each station, because knowing the time of arrival better helps to clearly identify the first motion. In particular, ad-

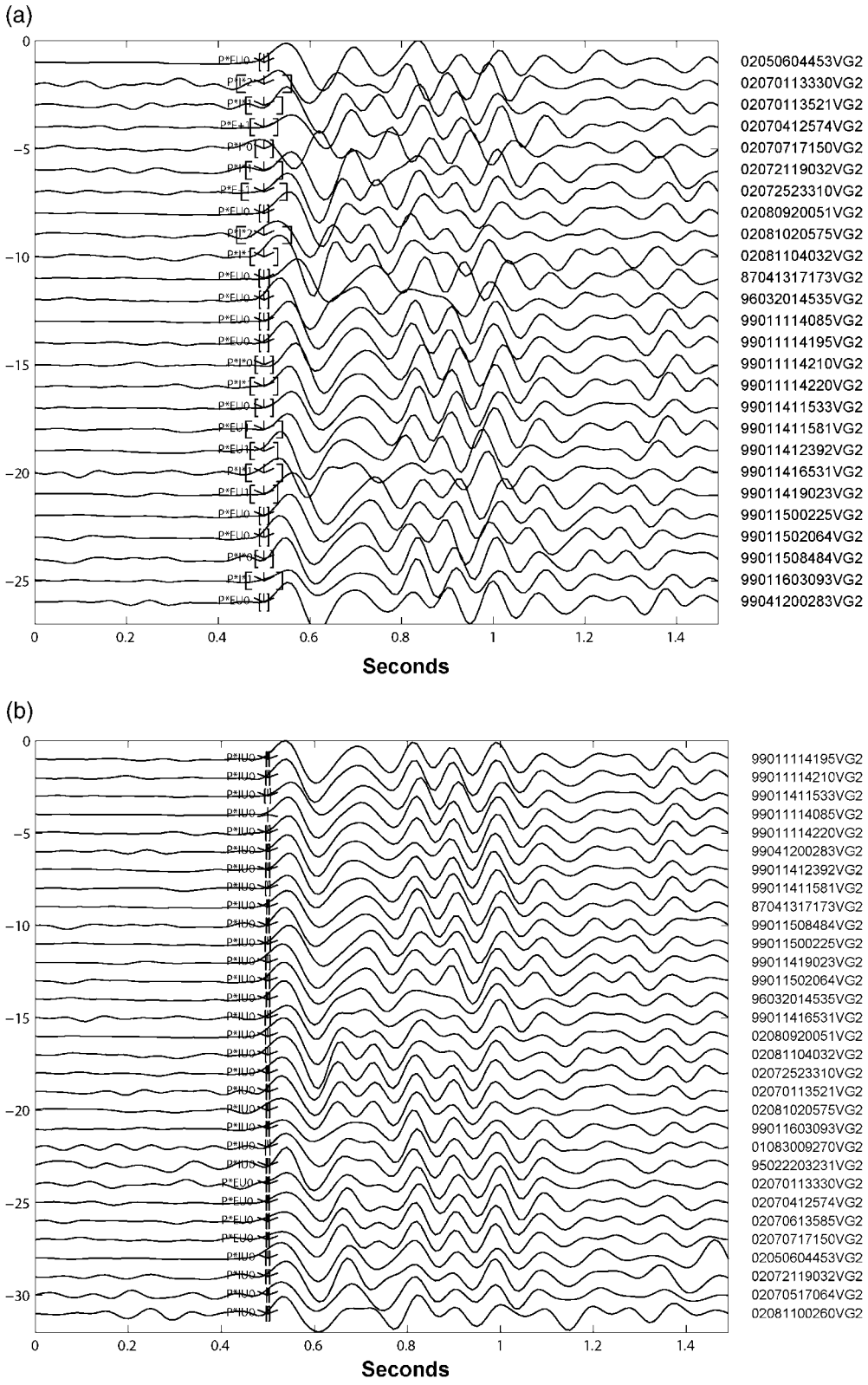

Figure 7. Sample group of 31 traces from station VG2, bandpass filtered at 2 and 14 Hz, before and after cross-correlation. (a) Catalog picks for 26 of 31 traces. (b) Adjusted picks.

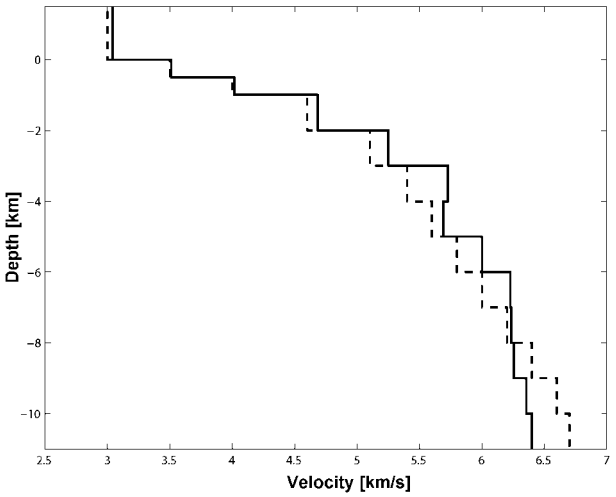

Figure 8. Initial (dashed line) and final (solid line) 1D velocity models obtained by solving the coupled hypocenter-velocity model problem. *P* picks for 89 earthquakes were used in this inversion.

ditional polarities can often be picked for intermediate-distance stations, where catalog picks are sometimes adjusted by 0.1 sec or more during cross-correlation.

After polarities were adjusted or assigned for all high-quality arrivals, first-motion focal mechanisms were computed for select events by using the grid-search program FPFIT of Reasenberg and Oppenheimer (1985). Mechanisms were computed for all events with more than ten measured polarities, then inspected visually. Because many events had polarity picks at unused stations, we down-weighted these catalog polarities. Mechanisms with large focal sphere gaps and multiple, drastically different best-fit mechanisms were discarded.

Selected focal mechanisms from Mount Hood earthquakes are plotted in Figure 10. We observe that most focal mechanisms vary only minimally from those computed by using catalog picks. Because very few catalog first motions change, we conclude that changes in focal mechanisms are caused by changes in location, in particular, earthquake depth. However, with the exception of the summit cluster, earthquake faulting is still almost uniformly normal, with some oblique normal events. The orientations of *P* and *T* axes show little variation as functions of hypocentral depth or time.

Catalog Statistics and Statistical Analysis

Earthquake relocations alone do not offer a complete picture of seismicity. Several statistical parameters provide additional insights into the cause of an earthquake sequence, such as the modified Omori's law *p*-value (Omori, 1894), and the *b*-value of the Gutenberg–Richter law (Gutenberg and Richter, 1956). We examine both *p*- and *b*-values for both the complete catalog and the summer 2002 earthquake swarm, with the Zmap program of Wiemer (2001), to supplement our knowledge of the spatial distribution and relative locations.

Because station coverage at Mount Hood was subject to periodic outages, and network sensitivity has been increased during the past several years, we expect that the PNSN has not detected small Mount Hood events uniformly over time. We investigate this by analyzing the distribution of the number of earthquakes, *N*, as a function of duration magnitude, using a form of the Gutenberg–Richter relationship,

$$\log_{10}(N) = a - bM_{\mathrm{D}}, \tag{1}$$

where N is the total number of earthquakes with duration magnitude M_{D} and b is a constant for the complete catalog. A typical effect of catalog incompleteness is unreliable detection of low-magnitude events. This appears as a slope decrease in a plot of $\log(N)$ vs. M_{D} at lower magnitudes. The magnitude threshold of completeness, M_{D}, is the lowest magnitude for which the relation remains a straight line. Applying this criterion to the Mount Hood earthquake catalog, we find that the minimum value for catalog completeness is M_{D} 0.9 (Fig. 11). By calculating the catalog completeness magnitude for overlapping ten-year time windows centered from 1986 through 1997, we find no significant change in this value with time. This suggests that the apparent increasing rate of seismicity is not a result of increased detection capability.

The *b*-value parameter itself is often useful in understanding the causes of an earthquake swarm. For most tectonic regions of the Earth, $b \leq 1.0$ (Minakami, 1990). However, active volcanic areas can have much larger *b*-values, often with $b \geq 1.5$, because of increased crack density and/or high pore pressure. Examples include Mt. Pinatubo, Philippines (Sanchez *et al.*, 2004), Ito, Japan (Wyss *et al.*, 1997), and Etna, Italy (Vinciguerra, 2002). The most common explanation for such high *b*-values is a weak, inhomogeneous crust, incapable of sustaining high strain levels and a heterogeneous stress system (Lay and Wallace, 1995, p. 439). Thus, the *b*-value parameter is an indirect measurement of crustal weakening or high localized strain rates such as might be caused by fluid movement or extensive networks of small fractures.

We compute the *b*-value for the summer 2002 earthquake sequence using the maximum-likelihood technique (Page, 1968). For this sequence we define all events between the 29 June 2002 mainshock and 31 July 2002 as "aftershocks." We find that the catalog completeness magnitude for this earthquake sequence is M_{D} 1.0, similar to the completeness magnitude for the entire Mount Hood catalog. The maximum-likelihood *b*-value for this sequence is determined to be 0.723 ± 0.08. This is similar to, or even lower than, *b*-values for other crustal earthquake sequences in the central Cascades. Examples include 0.88 ± 0.16 for Scotts' Mills (Thomas *et al.*, 1996), 0.77 ± 0.05 for Elk Lake (Grant *et al.*, 1984), and 0.67 ± 0.01 for deep Mount St. Helens post-eruption seismicity in 1980 (Weaver *et al.*, 1981).

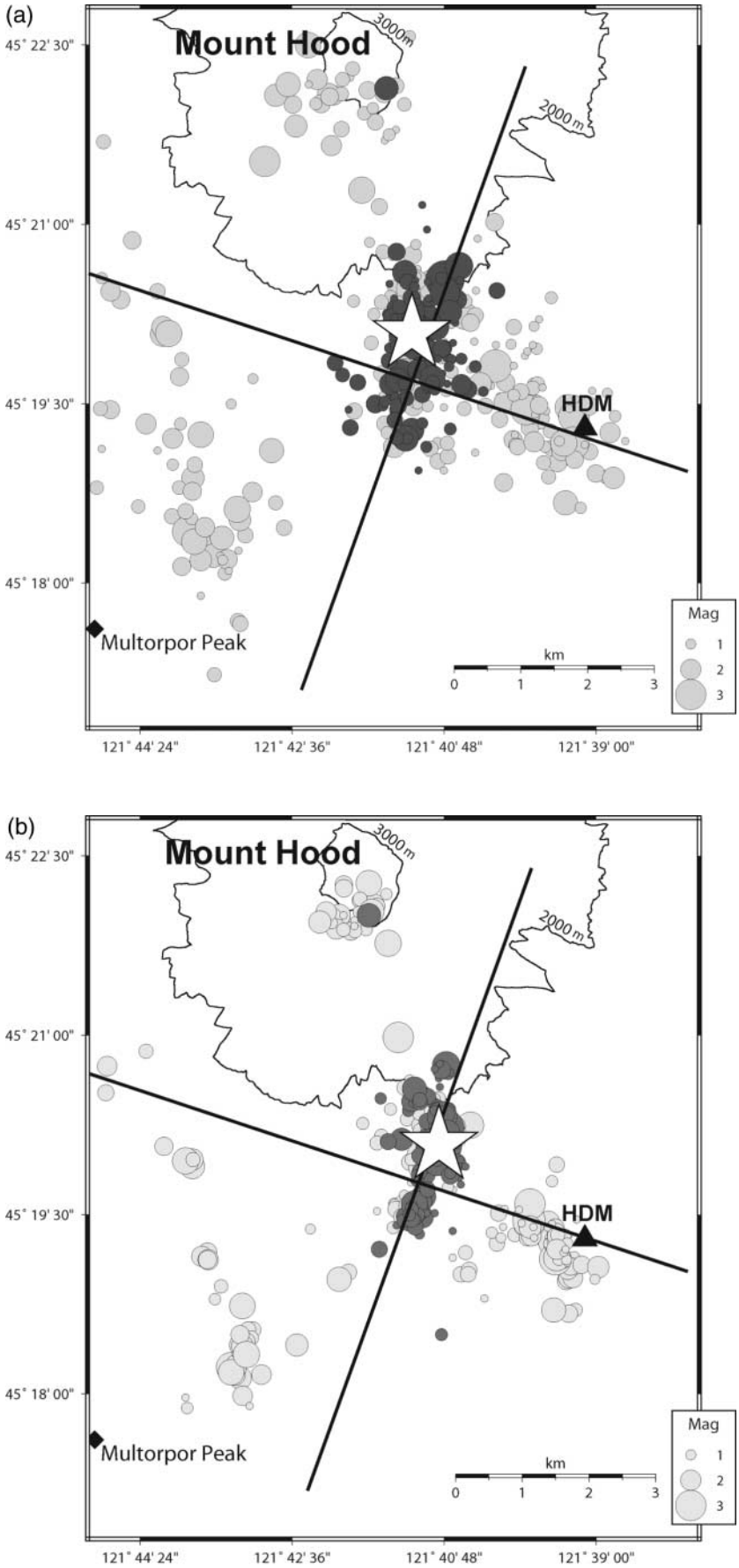

Figure 9. (a) Catalog epicenters for selected Mount Hood earthquakes. (b) Epicenters calculated using HypoDD (Waldhauser and Ellsworth, 2000) on catalog arrival-time picks. (c) Epicenters calculated using HypoDD on adjusted (cross-correlated) arrival-time picks. (d) Catalog hypocenters, rotated N15E. (e) Relocated hypocenters with catalog arrival times. (f) Relocated hypocenters with adjusted arrival times. On all plots, events from 2002 are indicated in dark gray, and older events appear in light gray. The 29 June 2002 mainshock (M_D 4.5) appears as a white star. Position of Mount Hood is indicated by contour lines and text on epicenter maps. Multorpor Peak is indicated with a black diamond and text. The temporary station HDM is indicated with a black triangle and station label on epicenter maps. In Figures 9a–9c, the cross sections for each corresponding pair of depth slices (9d–9f) are indicated with solid black lines. (*continued*)

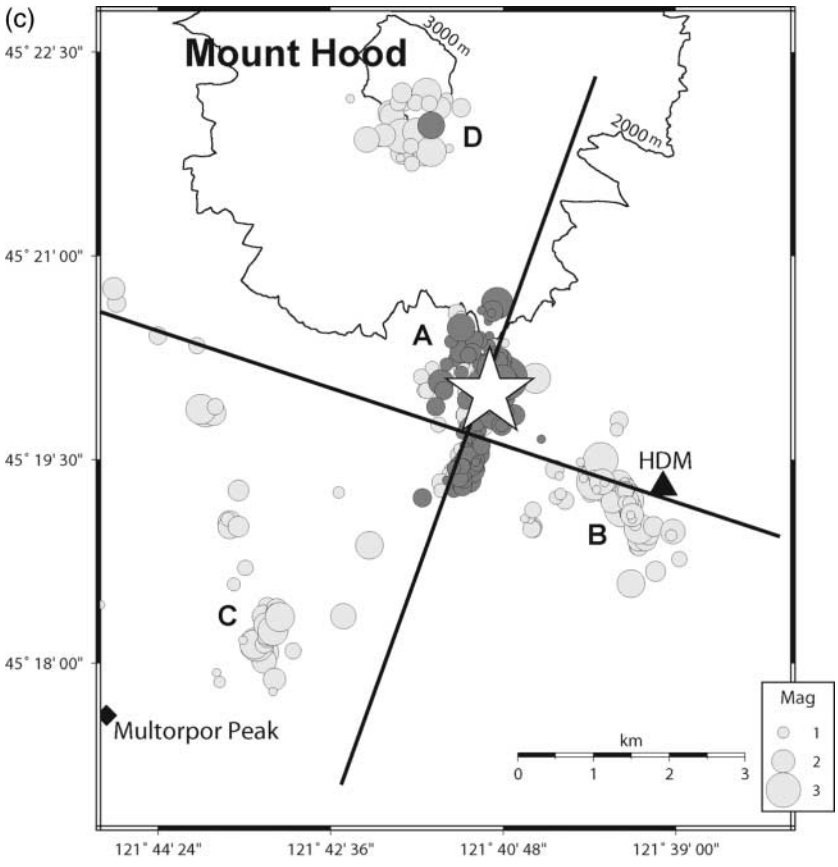

Figure 9. Continued.

Because changes in the *b*-value parameter with time are also indicators of potential unrest, we compute *b*-values in overlapping time windows, each containing 150 earthquakes, for earthquakes occurring between 1980 and 2002. The error associated with estimation of each *b*-value is calculated by using the formula of Shi and Bolt (1982):

$$\sigma(b) = \frac{2.3b^2\sqrt{\Sigma(M_i - \bar{M})^2}}{N(N-1)} \quad (2)$$

where $\bar{M}$ is the average of the magnitude for N seismic events, and M_i is the magnitude of the ith earthquake. We compute the *b*-value parameter as a function of time for events with $M_D > 0.9$. A simple, linear regression analysis of the data set (Fig. 12) shows only a slight increase with time but doesnot rise above typical values for tectonic earthquakes. Thus, although the *b*-value increased since 1986, it does not change significantly enough, nor rise high enough, to indicate potential for unrest.

Finally, we examine the *p*-value for the summer 2002 earthquake sequence. This parameter measures the rate of fall-off of aftershocks and is the decay constant of the modified Omori's Law,

$$n = \frac{C}{(K+t)^p}, \quad (3)$$

where n is the frequency of aftershocks at time t after the mainshock, and K and C are constants that depend on the size of the earthquake (Omori, 1894). For tectonic sequences the *p*-value is typically in the range 1.0–1.4 but has been measured as low as 0.75 for aftershock sequences in southern California (Reasenberg and Jones, 1989). Treating the M_D 4.5 earthquake as the mainshock, we calculate the *p*-value for the summer 2002 earthquake swarm as 0.82 ± 0.07, suggesting that this sequence decayed with time somewhat more slowly than most aftershock sequences.

Results and Discussion

After relocation, the two diffuse clusters of catalog seismicity separate into four distinct groups with resolvable structure. Most individual earthquake swarms take place within a single cluster. Only a few recent swarms have earthquakes in two groups or more. We discuss the spatial characteristics of each group separately, along with implications for the underlying processes responsible.

South Cluster A

More than 70% of relocatable events belong to a large cluster south and south-southeast of Mount Hood, striking roughly N15E, with a diffuse northern end and tighter southern region. This cluster is labeled A on Figure 9c. The spatial

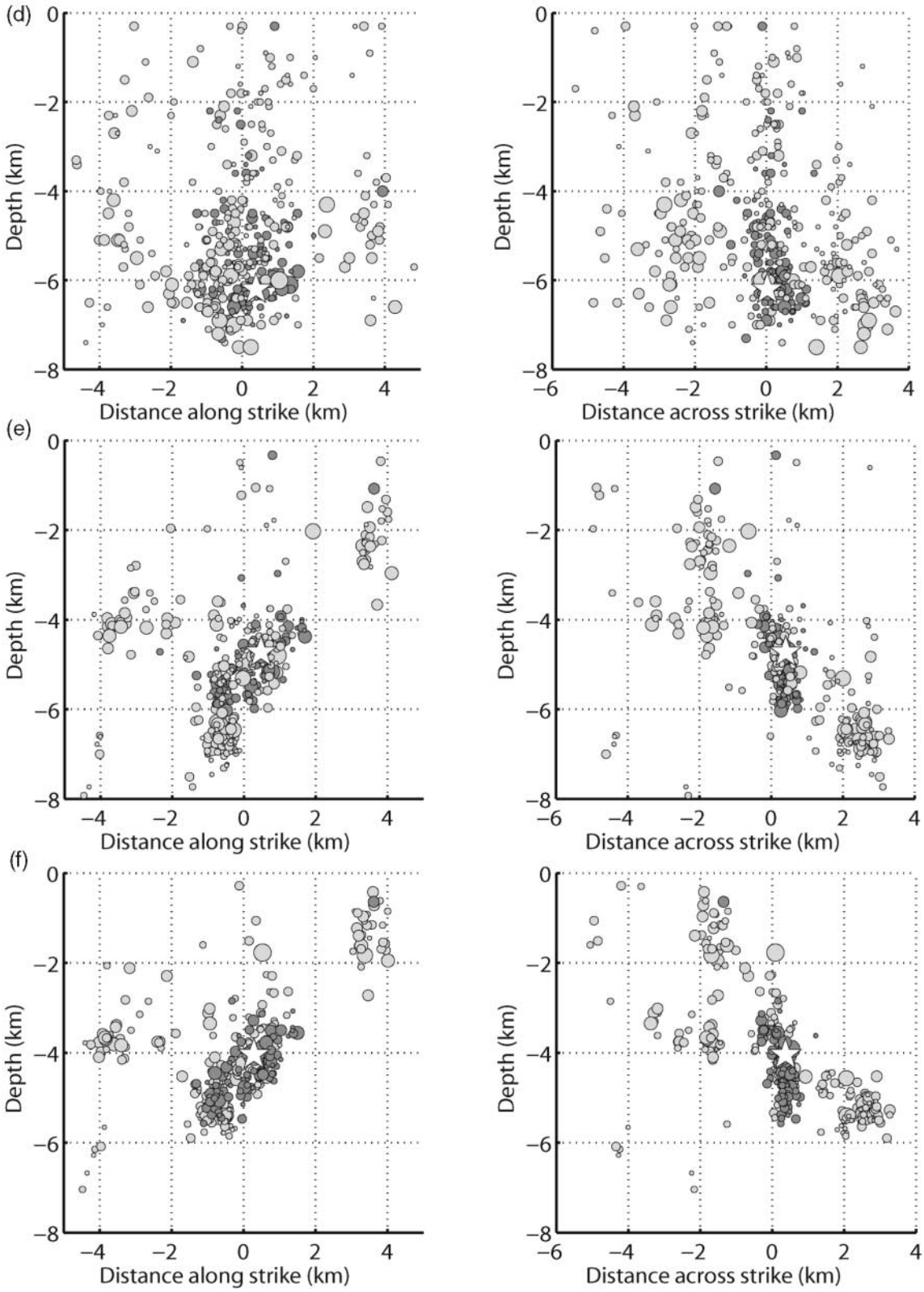

Figure 9. Continued.

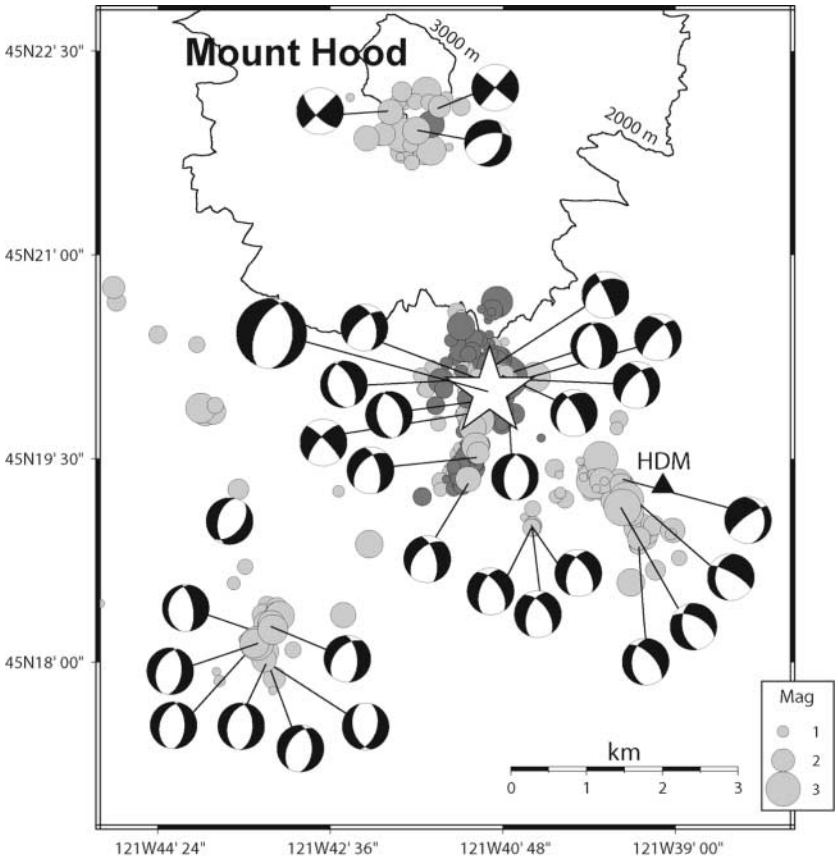

Figure 10. Selected first-motion focal mechanisms for Mount Hood earthquakes. Five focal mechanisms were removed from the plot because they corresponded to earthquakes in nearly identical positions, and with nearly identical mechanisms, to earthquakes whose focal mechanisms are already shown. The large mechanism corresponds to the M_D 4.5 earthquake of 29 June 2002. Epicenter colors are the same as Figure 9.

distribution of earthquakes is consistent with a steeply dipping normal fault (Fig. 9f). The existence of such a fault has been inferred before in roughly the same location from pseudogravity anomaly studies of aeromagnetic data (R. Blakely, unpublished data, 1984). However, if a fault does underlie Mount Hood at this location it has no geologically mapped surface expression. Inspection of the cross-sections for this cluster shows that the spatial distribution is in good agreement with the faulting inferred from first-motion focal mechanisms (Fig. 10). The relocated depths within this cluster increase with increasing distance from the summit. This detail is not obvious in catalog locations alone.

Southeast Cluster B

Further to the southeast, but still beneath the volcanic edifice, a diffuse group of smaller events collapses to a streak of seismicity trending N45W, labeled B (Fig. 9c). Events in this cluster occur at greater depths than closer clusters and depths change little with increasing distance from Mount Hood. Spatial distribution of hypocenters and uniformity of focal mechanisms with one nodal plane aligned along strike suggest that this cluster occurs on a fault in response to extensional stresses. However, earthquake swarms in this cluster do not follow typical mainshock-aftershock patterns, which are normally associated with tectonic origins. A good example is the swarm from January 1999 (Fig. 5), whose relocated hypocenters lie completely within this group. This feature corresponds closely to the White River fault identified from geologic evidence (Weaver *et al.*, 1982) suggesting that this fault is still active.

The south and southeast clusters do not appear connected. Apparently, an aseismic zone exists between the two clusters that was not obvious from catalog locations. The observation that no 2002 seismicity occurred in the southeast cluster despite its vigorous activity adds weight to the argument that these clusters represent activity on totally separate faults.

Southwest Clusters C

Approximately 10% of relocated events either belong to the southwest clusters or are isolated from any distinct cluster (labeled C on Fig. 9c). These appear spatially unrelated to seismicity beneath and south of the Mount Hood summit. Seismicity southwest of the summit is of interest because hypocenters collapse to much smaller volumes than could be surmised from catalog locations alone. Hypocentral depths range from 3.5 to 4.5 km, and epicenters align crudely along a linear feature striking N20W. The greatest concentration of seismicity occurs in a region 2–3 km east-northeast of Multorpor Peak and appears completely disconnected from other clusters. Focal mechanisms for these events are similar to those of events to the east. The uniformity of first-motion focal mechanisms suggests that some of the multiplets nearest the Multorpor cluster occur along the same (or

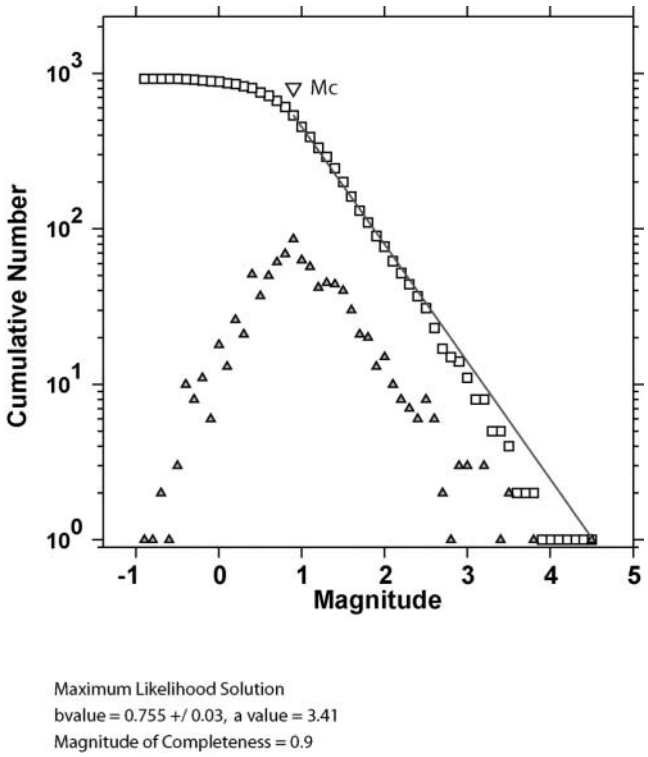

Figure 11. Catalog completeness plot, showing logarithmic magnitude vs. cumulative number of events, and maximum-likelihood *b*-value for entire Mount Hood catalog. White triangle indicates catalog completeness magnitude, M_D 0.9.

a parallel) fault. If some multiplets occur along the same fault as the Multorpor cluster, the inferred strike of this fault closely matches that of first-motion focal mechanisms. However, these earthquakes are much more tightly grouped than those in other Mount Hood clusters, and their spatial distribution does not closely match that of a normal fault. The cause of these earthquakes therefore remains an open question.

Summit Earthquakes D

The seismicity nearest the summit (labeled D on Fig. 9c) consists of very shallow microearthquakes (M_D <2.7) occurring over a volume of approximately 1 km^3. Hypocentral depths are shallower than for other clusters. Earthquakes here account for <10% of the total Mount Hood catalog seismicity. Although their spatial distribution is too scattered to suggest a magmatic conduit, they still might be associated with movement of fluids beneath the summit. Their circular distribution weakly supports the existence of a ring fault below the crater rim, as inferred by Friedman *et al.* (1982) from infrared data, but only if the fault extends to depths of 2–4 km below sea level. Because relative location errors are on the order of a few tens of meters, the distribution is clearly not an artifact of location scatter.

It is clear, from inspection of focal mechanisms (Fig. 10), that these earthquakes are being generated within a different stress regime than earthquakes elsewhere beneath the volcanic edifice and that the stress regime is less uniform than for other earthquake groups. These events, similar to shallow events directly under Mount Rainier (Giampiccolo *et al.*, 1999) and the shallow events at Mount St. Helens (Musumeci *et al.*, 2002) have distinct properties that are different than events away from their respective volcanoes: their shallow depths, nonuniform focal mechanisms, and diffuse distribution suggest that these earthquakes are likely generated by volcanic processes within and under Mount Hood.

Conclusions

The method of waveform cross-correlation and earthquake relocation has become a useful tool in understanding the spatial characteristics of earthquakes. Here, applied to largely ambiguous earthquake swarms from Mount Hood, we find that earthquakes occur in four distinctly separate groups, each with different implications for the state of stress

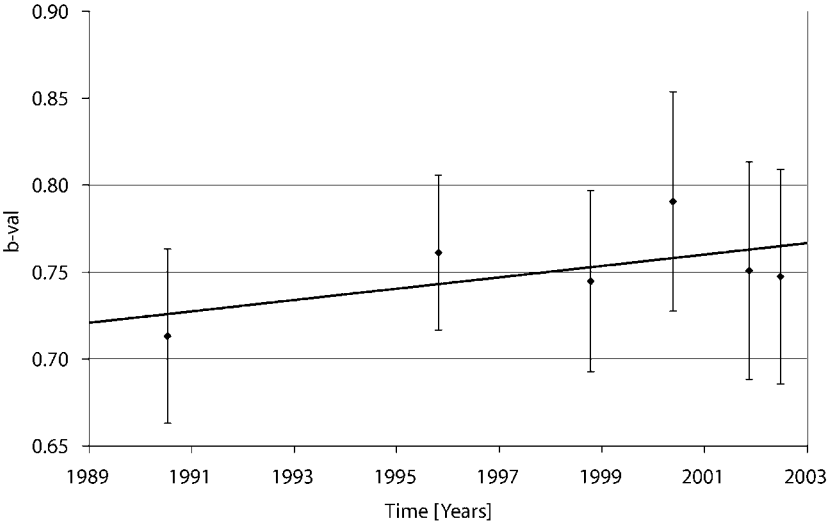

Figure 12. Change in *b*-value with time, showing best-fit linear regression line. *b*-values are computed in overlapping time windows, each containing 150 events, by using the maximum-likelihood method of estimation.

at the volcano. To the southwest, we observe several multiplets, including earthquakes approximately 2–3 km east-northeast of Multorpor Peak. Beneath Mount Hood summit is a small, shallow, diffuse cluster of earthquakes that may be the result of volcanic processes. The earthquakes south of Mount Hood occur along at least two separate, disconnected faults, the White River fault, and an unnamed, buried, steeply dipping normal fault, south of the summit.

The summer 2002 events clearly appear to be a typical mainshock-aftershock sequence occurring on this fault. The M_D 4.5 main shock, and all large ($M > 2.5$) aftershocks, occurred within this group. Focal mechanisms of 2002 events are almost uniformly normal, consistent with earlier earthquakes in the same area. The 2002 earthquakes follow a temporal pattern typical of tectonic aftershocks, as characterized by the *p*- and *b*-value parameters. These findings suggest that this sequence occurred in response to tectonic stresses acting on extended, weakened crust in the Mount Hood area.

We interpret the 2002 sequence as an example of Basin and Range extensional stress. This confirms the extension of the seismically active Basin and Range province into the transition zone between extensional and compressional dominated volcanism (Guffanti and Weaver, 1988). The idea that the High Cascades partially overlie the Basin and Range province is not new and is discussed in Williams *et al.* (1982). Mount Hood likely lies in a transition zone where the High Cascades partly overlie the Basin and Range, whose hot, extended crust is being subjected to both extensional tectonic stresses and stresses from isolated volcanic processes.

Although some ambiguity remains in the interpretation of older, smaller earthquake swarms, their *b*-values are consistently too small to infer that magma movement is likely responsible for even a significant fraction of earthquake activity. Although it is possible for VT earthquake sequences to be triggered by pressure increases caused by magma movement, we find no evidence that this is the case here; therefore, we conclude that the Mount Hood earthquakes do not suggest any serious potential for volcanic unrest at this time.

As a follow-up to this research, the temporary site HDM has been reoccupied and now holds a permanent, telemetered seismograph station, with broadband and strong-motion sensors. This new station, named HOOD, was added to the Pacific Northwest Seismic Network in early November 2002. We expect that the new station will greatly increase our understanding of earthquakes at Mount Hood by better constraining locations, providing more accurate hypocentral depths, and improving detection capabilities.

Acknowledgments

We thank the staff of the PNSN for their efforts to provide high-quality seismic recordings of earthquakes. We thank Robert Norris and Craig Weaver for insightful discussions, and Elizabeth Barnett and Robert Norris for invaluable assistance with installing the temporary station HDM. We thank Charlotte Rowe and two anonymous reviewers for their suggestions and comments, which have lead to improvement of this article. This research was funded, in part, by the U.S. Geological Survey Joint Operating Agreement 01-HQ-AG-0011.

References

Berg, J. W., Jr., and C. D. Baker (1963). Oregon earthquakes 1841 through 1958, *Bull. Seism. Soc. Am.* **53,** 95–108.

Couch, R., and M. Gemperle (1979). Gravity measurements in the area of Mount Hood, Oregon, in Geothermal Resource Assessment of Mount Hood, DOGAMI Open File Rept. 0-79-8, State of Oregon, Department of Geology and Mineral Industries, Portland, 137–189.

Crosson, R. S. (1976). Crustal structure modeling of earthquake data 1. Simultaneous least squares estimation of hypocenter and velocity parameters, *J. Geophys. Res.* **81,** no. 17, 3036–3046.

Deichman, N., and M. Garcia-Fernandez (1992). Rupture geometry from high-precision relative hypocenter locations of microearthquake ruptures, *Geophys. J. Int.* **110,** 501–517.

Dodge, D. A., G. C. Beroza, and W. L. Ellsworth (1995). Evolution of the 1992 Landers, California foreshock sequence and its implications for earthquake nucleation, *J. Geophys. Res.* **100,** 9865–9880.

Folsom, M. M. (1970). Volcanic eruptions: the pioneers attitudes on the Pacific Coast from 1800 to 1875, *Ore Bin* **32,** no. 4, 61–71.

Fremont, M. J., and S. D. Malone (1987). High precision relative locations of earthquakes at Mount St. Helens, Washington, *J. Geophys. Res.* **92,** 10,223–10,236.

Friedman, J. D., D. L. Williams, and D. Frank (1982). Structural and heat flow implications of infrared anomalies at Mt. Hood, Oregon, 1972–1977, *J. Geophys. Res.* **87,** no. B4, 2793–2803.

Giampiccolo, E., C. Musumeci, S. D. Malone, S. Gresta, and E. Privitera (1999). Seismicity and stress-tensor inversion in the central Washington Cascade Mountains, *Bull. Seism. Soc. Am.* **89,** 811–821.

Grant, W. C., C. S. Weaver, and J. E. Zollweg (1984). The 14 February 1981 Elk Lake, Washington, earthquake sequence, *Bull. Seism. Soc. Am.* **74,** 1289–1309.

Green, S. M., C. S. Weaver, and H. M. Iyer (1979). Seismic studies at the Mt. Hood volcano, northern Cascade range, Oregon. *U.S. Geol. Surv. Open-File Rept. 79-1691*.

Guffanti, M., and C. S. Weaver (1988). Distribution of lat Cenozoic volcanic vents in the Cascade Range; volcanic arc segmentation and regional tectonics, *J. Geophys. Res.* **93,** no. 6, 6513–6529.

Gutenberg, B., and C. Richter (1956). Earthquake magnitude, intensity, energy, and acceleration, *Bull. Seism. Soc. Am.* **46,** 105–145.

Kissling, E., W. L. Ellsworth, D. Eberhart-Phillips, and U. Kradolfer (1994). Initial reference models in local earthquake tomography, *J. Geophys. Res.* **99,** no. B10, 19,635–19,646.

Lahr, J. C., B. A. Chouet, C. D. Stephens, J. A. Power, and R. A. Page (1994). Earthquake location and error analysis procedures for a volcanic sequence: Application to 1989–1990 eruptions, *J. Volcanol. Geotherm. Res.* **62,** 137–152.

Lay, T., and T. C. Wallace (1995). *Modern Global Seismology*, Academic Press, San Diego.

Leaver, D. (1984). Mixed stochastic and deterministic modeling of the crustal structure in the vicinity of Mount Hood, Oregon. *Ph.D. Thesis*, University of Washington, Seattle.

Minakami, T. (1990). Prediction of volcanic eruptions, in *Physical Volcanology*, L. Civetta, P. Gasparini, G. Luongo, and A. Rapolla (Editors), Elsevier, Amsterdam, 1–27.

Musumeci, C., S. Gresta, and S. D. Malone (2002). Magma system recharge of Mount St. Helens from precise relative hypocenter location of microearthquakes, *J. Geophys. Res.* **107,** no. B10, 2264–2273.

Omori, F. (1894). On the aftershocks of earthquakes, *J. Coll. Sci. Imp. Univ. Tokyo* **7,** 111–216.

Page, R. (1968). Aftershocks and microaftershocks of the great Alaska earthquake of 1964, *Bull. Seism. Soc. Am.* **58,** 1131–1168.

Reasenberg, P., and D. Oppenheimer (1985). FPFIT, FPPLOT, and FPPAGE: FORTRAN computer programs for calculating and plotting earthquake fault-plane solutions, *U.S. Geol. Surv. Open-File Rept. 98-739*, 1109.

Reasenberg, P. A., and L. M. Jones (1989). Earthquake hazard after a mainshock in California, *Science* **243,** 1173–1176.

Rite, A., and H. M. Iyer (1981). July 1980 Mt. Hood earthquake swarm, *U.S. Geol. Surv. Open-File Rept. 81-48*.

Rowe, C. A., R. C. Aster, B. Borchers, and C. J. Young (2002). An automatic, adaptive algorithm for refining phase picks in large seismic data sets, *Bull. Seism. Soc. Am.* **92,** 1660–1674.

Rubin, A. M., D. Gillard, and J. L. Got (1998). A reinterpretation of seismicity associated with the January 1983 dike intrusion at Kilauea Volcano, Hawaii, *J. Geophys. Res.* **103,** no. B5, 10,003–10,015.

Sanchez, J. J., S. R. McNutt, J. A. Power, and M. Wyss (2004). Spatial variations in the frequency-magnitude distribution of earthquakes at Mt. Pinatubo volcano, *Bull. Seism. Soc. Am.* **94,** 430–438.

Shi, Y., and B. Bolt (1982). The standard error of the magnitude frequency b value, *Bull. Seism. Soc. Am.* **72,** 1677–1687.

Thomas, G. C., R. S. Crosson, D. L. Carver, and T. S. Yelin (1996). The 25 March 1993 Scotts Mills, Oregon, earthquake and aftershock sequence: spatial distribution, focal mechanisms, and the Mount Angel fault, *Bull. Seism. Soc. Am.* **84,** no. 4, 925–935.

Van Decar, J. C., and R. S. Crosson (1990). Determination of teleseismic relative phase arrival times using multi-channel cross-correlation and least squares, *Bull. Seism. Soc. Am.* **80,** no. 1, 150–169.

Vinciguerra, S. (2002). Damage mechanics preceding the September-October 1989 flank eruption at Mt. Etna volcano inferred by seismic scaling exponents, *J. Volcanol. Geotherm. Res.* **113,** 391–397.

Waldhauser, F., and W. L. Ellsworth (2000). A double-difference earthquake location algorithm: method and application to the northern Hayward fault, *Bull. Seism. Soc. Am.* **90,** 1353–1368.

Weaver, C. S., W. C. Grant, S. D. Malone, and E. T. Endo (1981). Post-May 18 seismicity: volcanic and tectonic implications, *U.S. Geol. Surv. Profess. Pap. 1250*, 109–121.

Weaver, C. S., S. M. Green, and H. M. Iyer (1982). Seismicity of Mount Hood and structure as determined from teleseismic *P* wave delay studies, *J. Geophys. Res.* **87,** no. B4, 2782–2792.

Westhusig, J. K. (1973). Reconnaissance surveys of near-event seismic activity in the volcanoes of the Cascade Range, Oregon, *Bull. Volcanol.* **37,** 1–29.

Wiemer, S. (2001). A software package to analyze seismicity: ZMAP, *Seism. Res. Lett.* **72,** no. 2, 373–382.

Williams, D. L., D. A. Hull, H. D. Ackermann, and M. H. Beeson (1982). The Mt. Hood region: volcanic history, structure, and geothermal energy potential, *J. Geophys. Res.* **87,** no. B4, 2767–2781.

Wise, W. S. (1969). Geology and petrology of the Mt. Hood area: a study of high Cascade volcanism, *Geol. Soc. Am. Bull.* **80,** 969–1006.

Wyss, M., K. Shimazaki, and S. Wiemer, (1997). Mapping active magma chambers by *b*-value beneath the off-Ito volcano, Japan, *J. Geophys. Res.* **102,** 20,413–20,422.

Department of Earth and Space Sciences
University of Washington
Seattle, Washington 98195-1310
josh@ess.washington.edu

Manuscript received 18 February 2004.